NETWORKS AND HETEROGENEOUS MEDIA
©American Institute of Mathematical Sciences
Volume **2**, Number **3**, September **2007**

Website: http://aimSciences.org

pp. **481–496**

ENSKOG-LIKE DISCRETE VELOCITY MODELS FOR VEHICULAR TRAFFIC FLOW

Michael Herty

AG Technomathematik, Fachbereich Mathematik
Universität Kaiserslautern
D-67663 Kaiserslautern, Germany

Lorenzo Pareschi

Department of Mathematics
University of Ferrara
I-44100 Ferrara, Italy

Mohammed Seaïd

AG Technomathematik, Fachbereich Mathematik
Universität Kaiserslautern
D-67663 Kaiserslautern, Germany

(Communicated by Axel Klar)

Abstract. We consider an Enskog-like discrete velocity model which in the limit yields the viscous Lighthill-Whitham-Richards equation used to describe vehicular traffic flow. Consideration is given to a discrete velocity model with two speeds. Extensions to the Aw-Rascle system and more general discrete velocity models are also discussed. In particular, only positive speeds are allowed in the discrete velocity equations. To numerically solve the discrete velocity equations we implement a Monte Carlo method using the interpretation that each particle corresponds to a vehicle. Numerical results are presented for two practical situations in vehicular traffic flow. The proposed models are able to provide accurate solutions including both, forward and backward moving waves.

1. **Introduction.** During the past decades several models have been proposed for mathematical studies on vehicular traffic flow, see for example [1, 2, 6, 8, 9, 14, 15, 16, 20] and further references are therein. These models present different techniques to describe dynamics of vehicles in a single road or networks. In the current work, we are interested in mathematical models derived from partial differential equations and also known by macroscopic models, compare [2, 5, 16, 19] among others. Recently, macroscopic models has also been applied to road networks by solving the associated partial differential equation on each arc (road) of the network, we refer the reader to [4, 11, 12, 13] for more details. The Lighthill-Whitham-Richards (LWR) model [16] is widely considered as one of the most simple models to describe vehicular traffic flow. It simplicity lies on the fact that the LWR equation is a scalar conservation law with strictly concave flux function which can be solved

2000 *Mathematics Subject Classification.* Primary: 65C05, 90B20; Secondary: 82B40.

Key words and phrases. Lighthill-Whitham-Richards model, Discrete-velocity equations, Monte Carlo method.

using well-established numerical methods. Therefore, the LWR model has become a prototype for theoretical and numerical investigations in vehicular traffic flow. As other mathematical equations for traffic flow, we cite the so-called 'second-order' models, see for instance [2, 5, 19].

The objective of the present study is to obtain a kinetic formulation for the LWR equation using only positive speeds and then to derive a Monte-Carlo method for its numerical treatment. The particles in the latter could then be interpreted as single cars of non–negative traveling speed. The Monte Carlo method has been successfully used in numerical solution of gas dynamics and has found many other applications, see [18] and other references can be found therein. However, to the best of our knowledge, this is the first time that Monte Carlo method is used to solve problems in traffic flow. There are two main reasons for considering this method. The first is that the Monte Carlo method can provide a fast and reliable computations for traffic flow and also a possible extension to networks. For instance, solving large scale traffic networks, fully discrete methods require tremendous computational effort. A Monte Carlo method however, allows to resolve different parts of the network by a different number of particles (samples) which their dynamic in the network can be obtained by solving the LWR or 'second-order' models. The second reason is that describing vehicles as particles, the Monte Carlo method can be interpreted as a natural way to describe uncertainty in the traffic behavior such as driver reactions. This stochastic effects in traffic flow can be easily incorporated in the Monte Carlo method.

The Monte Carlo algorithm proposed in this paper is based on a kinetic discrete velocity model proposed and studied by the authors in [10]. Here, we introduce a new formulation of traffic flow models including a "look-ahead" distance which yields an Enskog-like kinetic approximation. This discrete velocity model constitutes the basis of our Monte Carlo method. Numerical results and examples are carried out using the LWR equation, but our Monte Carlo method can be applied also to the 'second-order' Aw-Rascle model [2]. At the appropriate places we comment on possible extensions and modifications.

The outline of this paper is as follows. In section 2 we briefly describe the equations of vehicular traffic flow used to develop our Monte Carlo algorithm. The kinetic discrete velocity model is formulated in section 3. In section 4 we discuss the probabilistic Monte Carlo method for solving the kinetic equations. Numerical results for two test examples are presented in section 5. Section 6 summarizes the paper with concluding remarks.

2. **Traffic flow equations.**

For the sake of simplicity we formulate our Monte Carlo method for traffic flow models governed by partial differential equations of LWR type. However, all the derivations presented in this paper can be applied to 'second-order' traffic flow models without major conceptual modifications.

The LWR model requires only a state equation for traffic flow that relates the velocity to density and is mainly based on traffic observations. It is formulated by a scalar equation of conservation law written in dimensional form as

$$\rho_t + V(\rho)_x = 0, \tag{1}$$

where $\rho = \rho(x,t)$ is the density of vehicles at position x and time t. The flux function $V(\rho)$, which may depend on space x as well, is defined by

$$V(\rho) = \rho v_e(\rho), \tag{2}$$

where $v_e(\rho)$ is an equilibrium velocity known in traffic flow terminology by the fundamental diagram. The fundamental diagram is a necessary condition to describe the rate relationship between density and flow fields. In most applications, it is determined by empirical evidence of traffic behaviour. A well-established choice for the fundamental diagram $v_e(\rho)$ is

$$v_e(\rho) = v_m \left(1 - \frac{\rho}{\rho_m}\right), \tag{3}$$

with ρ_m and v_m are the maximum density and the maximum speed, respectively. Since it is more convenient to work with non-dimensional model than its dimensional counterpart, we define the following non-dimensional variables

$$t^* = \frac{Lt}{v_m}, \qquad x^* = \frac{x}{L}, \qquad \rho^* = \frac{\rho}{\rho_m}, \qquad v^* = \frac{v}{v_m},$$

where L denotes the length of the traffic road. Hence, the dimensionless equations governing the LWR model (1) can be rewritten as

$$\rho_t + V(\rho)_x = 0, \tag{4}$$

where we have dropped the asterisk of the dimensionless variables for ease of notation. The dimensionless flux function in (2) becomes

$$V(\rho) = \rho\,(1 - \rho)\,. \tag{5}$$

Thus, the equations (4)-(5) has to be solved in the spatial domain $[0, 1]$ and time interval $[0, T]$ subject to a given initial condition

$$\rho(x, 0) = \rho_0(x). \tag{6}$$

It is easy to verify that the non-dimensional density satisfies

$$0 \le \rho(x, t) \le 1. \tag{7}$$

Note that more general flux functions can also be incorporated in the following discussions. Motivated by the ideas reported in [10] we introduce a class of discrete velocity models as an approximation of equations (4)-(6). It should be stressed that, for traffic flow in networks, fast numerical methods are usually required for the treatment of possibly high dimensions of the problem, compare [12, 13] for some examples. In the present study, we consider the simple discrete velocity model proposed in [10] for vehicular traffic flow. This Enskog-type kinetic model contains only positive velocities and accounted for a "look-ahead" concept to recover backward waves in traffic dynamics. In addition, the discrete velocity model asymptotically preserves the "correct" LWR limit. A Monte Carlo method is developed based on the considered kinetic model and is formulated for the LWR model. However, this approach also applies to the second-order models in traffic flow, see Remark 3.2.

3. **Enskog-like discrete velocity model.**

Discrete velocity models for vehicular traffic flow have been studied by the authors in [10]. In this reference, we have proposed a class of two- and three-speed discrete velocity models with positive speeds only. Deterministic methods based on relaxation discretization and implicit-explicit schemes were used to approximate numerical solutions to the kinetic discrete velocity models. In the current work, we propose a different approach to reconstruct kinetic models for traffic flow with positive finite speeds. The emphasis is given to a two-speed kinetic model for the LWR problem in a single road. In contrast to discrete velocity models derived in [10], the proposed model incorporate the concept

of "look-ahead" principle in its formulation. This property avoids some limitations concerned with *subcharacteristic* conditions and fits with the frame of "follow the leader" in traffic flow modelling.

3.1. **Two speed models.** Let us consider two nonnegative speeds v_1 and v_2, and kinetic variables $f(x,t)$ and $g(x,t)$ corresponding to vehicles or particles with speed v_1 and v_2, respectively. Without loss of generality, we assume

$$0 \le v_1 < \frac{V(\rho)}{\rho} < v_2. \tag{8}$$

We define the (vehicle-)density ρ and the flux J as

$$\begin{aligned} \rho(x,t) &= f(x,t) + g(x,t), \\ J(x,t) &= v_1 f(x,t) + v_2 g(x,t). \end{aligned} \tag{9}$$

A discrete Enskog model for the kinetic variables f and g reads

$$f_t(x,t) + v_1 f_x(x,t) = -\frac{1}{\epsilon}\Big(f(x,t)E_g(x+h,t) - g(x,t)E_f(x+h,t)\Big), \tag{10}$$

$$g_t(x,t) + v_2 g_x(x,t) = -\frac{1}{\epsilon}\Big(g(x,t)E_f(x+h,t) - f(x,t)E_g(x+h,t)\Big), \tag{11}$$

where $\epsilon > 0$ is the relaxation time and $h > 0$ is the "look-ahead" distance. The equilibrium states $E_f(x,t) = E_f\left(\rho(x,t)\right)$ and $E_g(x,t) = E_g\left(\rho(x,t)\right)$ are implicitly defined according to

$$\begin{aligned} f + g &= \rho, \\ v_1 f + v_2 g &= J = V(\rho), \end{aligned} \tag{12}$$

and therefore, fulfill

$$\begin{aligned} E_f(x,t) &= \frac{\rho(x,t)}{v_2 - v_1}\left(v_2 - \frac{V(\rho(x,t))}{\rho(x,t)}\right), \\ E_g(x,t) &= \frac{\rho(x,t)}{v_2 - v_1}\left(\frac{V(\rho(x,t))}{\rho(x,t)} - v_1\right). \end{aligned} \tag{13}$$

Note that by virtue of (12) the kinetic system can be written as

$$f_t(x,t) + v_1 f_x(x,t) = -\frac{1}{\epsilon}\Big(\rho(x+h,t)f(x,t) - \rho(x,t)E_f(x+h,t)\Big), \tag{14}$$

$$g_t(x,t) + v_2 g_x(x,t) = -\frac{1}{\epsilon}\Big(\rho(x+h,t)g(x,t) - \rho(x,t)E_g(x+h,t)\Big). \tag{15}$$

For notational convenience we set $\rho^h = \rho(x+h,t)$ and similarly for E_f^h and E_g^h. Next, before we discuss properties of the model (10)-(11) and derive the viscous LWR limit, the kinetic model (10)-(11) can be interpreted as follows. According to condition (8) and due to equation (10), slower vehicles will speed up depending on the number of fast vehicles in the next cell *i.e.*, at position $x+h$. In fact, the loss term in equation (10) is fE_g^h and therefore the loss is *not proportional* to the actual number of fast vehicles (g^h) but, to the number of fast vehicles being in the equilibrium E_g^h. Similarly, the gain term for (10) is gE_f^h and therefore, vehicles of fast speed will slow down proportionally to the number of vehicles in the next cell

assumed to be at the equilibrium. The parameter h describes therefore the "look-ahead" distance. These ideas are inspired from an Enskog-like modelling taking into account the size of the interacting particles.

From (10)-(11) we formally obtain the following macroscopic equations

$$\rho_t + J_x = 0, \tag{16}$$

$$J_t + (v_1 + v_2)J_x - v_1 v_2 \rho_x = -\frac{1}{\epsilon}\left(\rho^h J - \rho V(\rho^h)\right). \tag{17}$$

In the zeroth order expansion for ϵ, the above equations yield

$$\rho_t + \left(\frac{\rho}{\rho^h} V(\rho^h)\right)_x = 0. \tag{18}$$

In the case of the flux function (5) and for small values of h ($h \ll 1$) we obtain the viscous LWR equation

$$\rho_t + (\rho(1-\rho))_x = \frac{h}{2}\left(\rho^2\right)_{xx} + \mathcal{O}(h^2). \tag{19}$$

Hence, in the small relaxation limit $\epsilon \longrightarrow 0$ and for small "look-ahead" distance $h \ll 1$, the two-speed discrete velocity model (10)-(11) is an approximation for the LWR equation with an additional diffusive term *i.e*, it approximately solves

$$\rho_t + (\rho(1-\rho))_x = \frac{h}{2}\left(\rho^2\right)_{xx}. \tag{20}$$

For a more general flux function of the form $V(\rho) = \rho v(\rho)$ the same asymptotic analysis leads to the approximate equation

$$\rho_t + (\rho v(\rho))_x = -h\left(v'(\rho)\rho_x\right)_x, \tag{21}$$

which is dissipative provided the condition $v'(\rho) < 0$ is satisfied. We end the modelling part with the following remarks:

Remark 1. First, compared to other discrete velocity models as those proposed for example in [17, 10], there is no condition necessary to ensure the dissipative nature of (10)-(11). In other words, no *subcharacteristic* condition is required for its stability.

Second, discrete velocity models with more than two speeds can also be derived. For a M speeds v_m with $M > 2$ and the kinetic variables f_m the general form is then

$$\partial_t f_m + v_m \partial_x f_m = -\frac{1}{\epsilon}\left(f_m \rho^h - \rho E^h_{f_m}\right), \qquad m = 1, \ldots, M, \tag{22}$$

where the equilibrium distributions E_{f_m} are defined such that

$$\begin{aligned} \sum_{m=1}^{M} E_{f_m} &= \rho, \\ \sum_{m=1}^{M} E_{f_m} v_m &= V(\rho). \end{aligned} \tag{23}$$

Note that, except for the case of $M = 2$, the constraints (23) are not sufficient to derive unique expressions for E_{f_m}. As in the classical BGK model for gas dynamics, additional conservation laws might be introduced to obtain uniqueness.

3.2. **Four speed models.** Another class of models arising in the literature on traffic flow are so called 'second-order' models. They consist of a 2x2 system of conservation laws and have been derived by borrowing ideas from gas dynamic approaches and apply them to traffic flow. We refer the reader to [2, 19] a discussion of the various approaches. One recent model is the Aw-Rascle (AR) model proposed in [2]. This model has several advantages over the previously proposed models, *e.g.* Payne-Whitham, and has been under investigation for several years [2, 7, 14]. Written in a conservative form, the AR model is given by

$$\begin{aligned} \rho_t + \left(\rho v(\rho, y)\right)_x &= 0, \\ y_t + \left(y v(\rho, y)\right)_x &= 0, \end{aligned} \tag{24}$$

where ρ is the total density of cars and

$$\rho\, v(\rho, y) = y - \rho\, p(\rho).$$

As stated in [2] there is no physical interpretation of the 'momentum' variable y in (24). However, the quantity $w = y/\rho$ is invariant in the mass-Lagrangian coordinate system and hence may be interpreted as "quality" (e.g. color) of a specific car. The pressure term $p(\rho)$ is an anticipation factor that takes into account drivers reactions to the state of traffic in front of them. It has to satisfy the following assumptions:

(i) $p(\rho) \approx \rho^\gamma$, for $\rho \to 0$ with $\gamma > 0$.

(ii) $\rho p''(\rho) + 2p'(\rho) > 0$, for all ρ.

There are many ways to reconstruct discrete velocity models associated with the AR traffic flow model. Here, we propose a kinetic discrete velocity model with four speeds given by the following equations

$$\begin{aligned} f_t + v_1 f_x &= -\frac{1}{\varepsilon}\Big(f(x,t)E_g(x+h,t) - g(x,t)E_f(x+h,t)\Big), \\ g_t + v_2 g_x &= -\frac{1}{\varepsilon}\Big(g(x,t)E_f(x+h,t) - f(x,t)E_g(x+h,t)\Big), \\ k_t + v_3 k_x &= -\frac{1}{\varepsilon}\Big(k(x,t)E_j(x+h,t) - j(x,t)E_k(x+h,t)\Big), \\ j_t + v_4 j_x &= -\frac{1}{\varepsilon}\Big(j(x,t)E_k(x+h,t) - k(x,t)E_j(x+h,t)\Big), \end{aligned} \tag{25}$$

where ε is the relaxation time, $h > 0$ is the "look-ahead" distance, v_i $(i = 1, \dots, 4)$ are nonnegative speeds, and f, g, k and j are the kinetic variables assumed to travel with speeds v_1, v_2, v_3 and v_4, respectively. Again, we assume without loss of generality

$$v_2 > v(\rho, y) > v_1 \geq 0 \qquad \text{and} \qquad v_4 > v(\rho, y) > v_3 \geq 0.$$

The equilibrium states E_f, E_g, E_k and E_j are defined according to

$$\begin{aligned} E_f + E_g &= \rho, \\ E_k + E_j &= y, \\ v_1 E_f + v_2 E_g &= \rho v(\rho, y), \\ v_3 E_k + v_4 E_j &= y v(\rho, y), \end{aligned} \tag{26}$$

Following the same procedure as in the LWR model, the equilibrium states can be explicitly calculated as

$$\begin{aligned} E_f &= \frac{\rho}{v_2 - v_1}\left(v_2 - v(\rho, y)\right), \qquad & E_g &= \frac{\rho}{v_2 - v_1}\left(v(\rho, y) - v_1\right), \\ E_k &= \frac{y}{v_4 - v_3}\left(v_4 - v(\rho, y)\right), \qquad & E_j &= \frac{y}{v_4 - v_3}\left(v(\rho, y) - v_3\right). \end{aligned} \tag{27}$$

In addition, the associated macroscopic model to (25) reads

$$\begin{aligned} \rho_t + J_x &= 0, \\ y_t + W_x &= 0, \\ J_t + (v_1 + v_2)J_x - v_1 v_2 \rho_x &= -\frac{\rho^h}{\varepsilon}\Big(J - \rho v(\rho^h, y^h)\Big), \\ W_t + (v_3 + v_4)W_x - v_3 v_4 y_x &= -\frac{y^h}{\varepsilon}\Big(W - y v(\rho^h, y^h)\Big), \end{aligned} \tag{28}$$

where $\rho = f + g$, $y = k + j$, $J = v_1 f + v_2 g$ and $W = v_3 k + v_4 j$.

In the leading order for small ε the equations (28) reduces to

$$\begin{aligned} \rho_t + \big(\rho v(\rho^h, y^h)\big)_x &= 0, \\ y_t + \big(y v(\rho^h, y^h)\big)_x &= 0. \end{aligned} \tag{29}$$

For small values of h, using a Taylor expansion one gets up to $\mathcal{O}(h^2)$ the approximate system

$$\begin{aligned} \rho_t + \left(\rho v(\rho, y)\right)_x &= -h\left(\rho v(\rho, y)_x\right)_x, \\ y_t + \left(y v(\rho, y)\right)_x &= -h\left(y v(\rho, y)_x\right)_x. \end{aligned} \tag{30}$$

The above system is parabolic if the diffusion matrix

$$\begin{pmatrix} -\rho v(\rho, y)_\rho & -\rho v(\rho, y)_y \\ -y v(\rho, y)_\rho & -y v(\rho, y)_y \end{pmatrix} \tag{31}$$

has nonnegative eigenvalues. A simple computation shows that the eigenvalues of (31) are given by

$$\lambda_1 = -\rho v(\rho, y)_\rho - \rho v(\rho, y)_\rho = \rho p'(\rho), \qquad \lambda_2 = 0,$$

and thus the parabolicity condition is fulfilled if $p'(\rho) > 0$.

Remark 2. The physical interpretation of the above four speed discrete velocity model is less straightforward then in the LWR case. Here we do not advocate the validity of the discrete velocity kinetic model for large values of the relaxation parameter but only in the limit as a tool for the construction of the Monte Carlo method. The development of more realistic four speeds models is actually under consideration.

4. Probabilistic Monte Carlo method.

To solve numerically the discrete velocity kinetic models proposed in the previous section we apply a Monte Carlo method previously applied to Boltzmann equation [18], rarefied gas dynamics [3], and Burgers equation [17]. Our method is asymptotic preserving, simple to implement and

approximate solution to the kinetic model with zero numerical viscosity. To simplify the presentation we restrict ourselves to the LWR case. The AR model can be treated in a similar way.

We start from the two speed model written in the form (14)-(15). Then, to solve numerically the system we split the problem into two stages.

(1) The transport stage

$$\begin{aligned} f_t + v_1 f_x &= 0, \\ g_t + v_2 g_x &= 0. \end{aligned} \tag{32}$$

(2) The relaxation stage

$$\begin{aligned} f_t &= -\frac{1}{\epsilon}\Big(f\rho^h - E_f^h\rho\Big), \\ g_t &= -\frac{1}{\epsilon}\Big(g\rho^h - E_g^h\rho\Big). \end{aligned} \tag{33}$$

Again, due to the Enskog-like interaction terms, no *subcharacteristic* condition is needed. However, to have a probabilistic interpretation of the above variables, we should have

$$f \geq 0, \qquad g \geq 0, \qquad \frac{f}{\rho} + \frac{g}{\rho} = 1,$$

which, at the limit ($\epsilon \longrightarrow 0$), is equivalent to impose

$$v_1 \leq \frac{V(\rho)}{\rho} \leq v_2.$$

To discretize the equations (32)-(33) in time we divide the time interval into subintervals $[t_n, t_{n+1}]$ with $t_n = n\Delta t$ and we denote by ψ^n the value of a generic function ψ at time t_n. During the relaxation stage we have $\rho(x, t_{n+1}) = \rho(x, t_n)$ and similarly for ρ^h. Hence, we can integrate the relaxation step exactly and obtain

$$\begin{aligned} f(x, t_{n+1}) &= (1-\lambda) f(x, t_n) + \lambda \frac{E_f^h(\rho(x, t_n))\rho(x, t_n)}{\rho^h(x, t_n)}, \\ g(x, t_{n+1}) &= (1-\lambda) g(x, t_n) + \lambda \frac{E_g^h(\rho(x, t_n))\rho(x, t_n)}{\rho^h(x, t_n)}, \end{aligned} \tag{34}$$

where λ is given by

$$\lambda = 1 - e^{-\frac{\Delta t}{\epsilon}\rho^h(x, t_n)}. \tag{35}$$

It is obvious from (35) that $0 \leq \lambda \leq 1$. Now let us define the probability density at time t_n as follows

$$P^n(\xi) = \begin{cases} \dfrac{f^n}{\rho^n}, & \text{if} \quad \xi = v_1, \\ \dfrac{g^n}{\rho^n}, & \text{if} \quad \xi = v_2, \\ 0, & \text{elsewhere.} \end{cases}$$

Note that $0 \leq P^n(\xi) \leq 1$ and $\sum_\xi P^n(\xi) = 1$. Moreover

$$\sum_\xi P^{n+1}(\xi) = \sum_\xi P^n(\xi) = 1.$$

The system (33) can be seen as an evolution of the probability function $P^n(\xi)$ according with

$$P^{n+1}(\xi) = \begin{cases} (1-\lambda)\dfrac{f^n}{\rho^n} + \lambda\dfrac{\rho^n}{\rho^{h,n}}E_f^h(\rho^n), & \text{if} \quad \xi = v_1, \\ (1-\lambda)\dfrac{g^n}{\rho^n} + \lambda\dfrac{\rho^n}{\rho^{h,n}}E_g^h(\rho^n), & \text{if} \quad \xi = v_2, \\ 0, & \text{elsewhere.} \end{cases} \tag{36}$$

Let $\{\xi_1, \xi_2, \ldots, \xi_N\}$ be the particle samples, we know that $\xi_j = v_1$ or $\xi_j = v_2$ with probability f^n/ρ^n or g^n/ρ^n, respectively. We also have the relation

$$P^{n+1}(\xi) = (1-\lambda)P^n(\xi) + \lambda E^n(\xi), \tag{37}$$

where $E^n(\xi)$ is defined as

$$E^n(\xi) = \begin{cases} \dfrac{\rho^n}{\rho^{h,n}}E_f(\rho^n), & \text{if} \quad \xi = v_1, \\ \dfrac{\rho^n}{\rho^{h,n}}E_g(\rho^n), & \text{if} \quad \xi = v_2, \\ 0, & \text{elsewhere.} \end{cases}$$

Hence, the relaxation stage (33) can be solved in the following way.

1. *Given a particle sample ξ the evolution of the sample during a time integration process is performed according to:*

   i. *With probability $(1-\lambda)$ the sample is unchanged.*

   ii. *With probability λ the sample is replaced with a sample from $E^n(\xi)$.*

2. *To sample a particle from $E^n(\xi)$ we proceed as follows:*

   i. *With probability $E_f(\rho)$ take $\xi = v_1$.*

   ii. *With probability $E_g(\rho)$ take $\xi = v_2$.*

To generate particles, we first divide the spatial domain into a finite sequence of cells $I_i = [x_{i-\frac{1}{2}}, x_{i+\frac{1}{2}}]$ with uniform stepsize Δx and centered in the gridpoint x_i. Then particles are generated from a given piecewise constant initial data in each cell and are randomly distributed around the cell center x_i. A simple way to carry this step out is to evaluate the histograms of samples on the cells I_i. For a set of N samples $p_1, p_2, \cdots, p_N$, we define the associated discrete probability density located at the gridpoint x_i by

$$p(x_i) = \frac{1}{N}\sum_{j=1}^{N}\frac{\delta_{I_i}(p_j - x_i)}{\Delta x}, \tag{38}$$

where $\delta_{I_i}(x)$ is the Kronecker delta function defined as

$$\delta_{I_i}(x) = \begin{cases} 1, & \text{if} \quad x \in I_i, \\ 0, & \text{elsewhere.} \end{cases}$$

Once the particle distribution is updated by the above steps, the transport stage of the splitting (32) is realized by advecting the position of the particles according to their speeds as

$$\begin{aligned} f_i^{n+1} &= f\left(x_i - v_1 \Delta t, t_n\right), \\ g_i^{n+1} &= g\left(x_i - v_2 \Delta t, t_n\right). \end{aligned} \tag{39}$$

Thus, given a sample of N particles at positions $x_1^n, x_2^n, \cdots, x_N^n$ and speeds $\xi_1, \xi_2, \cdots, \xi_N$ (equal either to v_1 or v_2) the new position of the particle sample $\{x_i^{n+1}, \xi_i\}$ is simply

$$x_i^n = x_i^{n+1} + \xi_i \Delta t, \qquad i = 1, \ldots, N,$$

where x_i^{n+1} and x_i^n are respectively, the new and old positions of the sample ξ_i. To summarize, Figure 1 illustrates the flow chart of the proposed Monte Carlo approach for the kinetic discrete velocity model (10)-(11).

Remark 3. Some remarks are in order:

1. Note that the splitting implemented in the present work is first-order accurate. For moderate stiff values of the relaxation parameter an extension of this approach to second-order accuracy can be realized by using a second-order Strang splitting together with a second-order reconstruction method based on particles in the spatial cells. It is still an open problem how to achieve second order accuracy in the limit $\epsilon \to 0$.
2. It is worth remarking that the proposed Monte Carlo method is mass conservative and preserves positivity of the solution variables without requiring any conditions on the selection of time steps.
3. As it is common in most Monte Carlo methods, we mainly need a random generator, particles sampling, stochastic rounding, counting and sorting procedures. All these technical tools have been studied with details in the lecture notes [18] to construct a Monte Carlo algorithm for the Boltzmann equation. In our Monte Carlo algorithm we have employed the same techniques.
4. Four samples of particles will be required for the Aw-Rascle model instead of the two samples used for the LWR model. The advection of samples are carried out according to their speeds and the projection to the equilibrium is performed using the probabilistic interpretation of the system (25).

5. **Numerical results and examples.** In this section we present numerical results for two test cases on traffic flow namely, free traffic and traffic jam situations. In all our computations we used a space interval $[-5, 5]$ discretized into 200 grid-points with uniform stepsize $\Delta x = 0.05$. The time step $\Delta t = 0.9\Delta x$ is selected and the number of particles is set to $N = 10^4$ which is large enough to decrease the stochastic effects in the obtained solutions. We perform numerical tests using the system (10)-(11) with two speeds chosen as $v_1 = 0$, $v_2 = 1$ and fixed "look-ahead" distance $h = \Delta x$. Other choices for the speeds are also possible. Here, we present only results for the relaxed case corresponding to $\epsilon = 0$. All the solutions presented here are reconstructed in similar manner as in (38) by averaging the number of particles in each cell *i.e.*,

$$\rho(x_i, t) = \frac{n(x_i, t)}{N \Delta x} \sum_{x_j \in I_i} \rho_0(x_j), \qquad i = 1, 2, \ldots, 200,$$

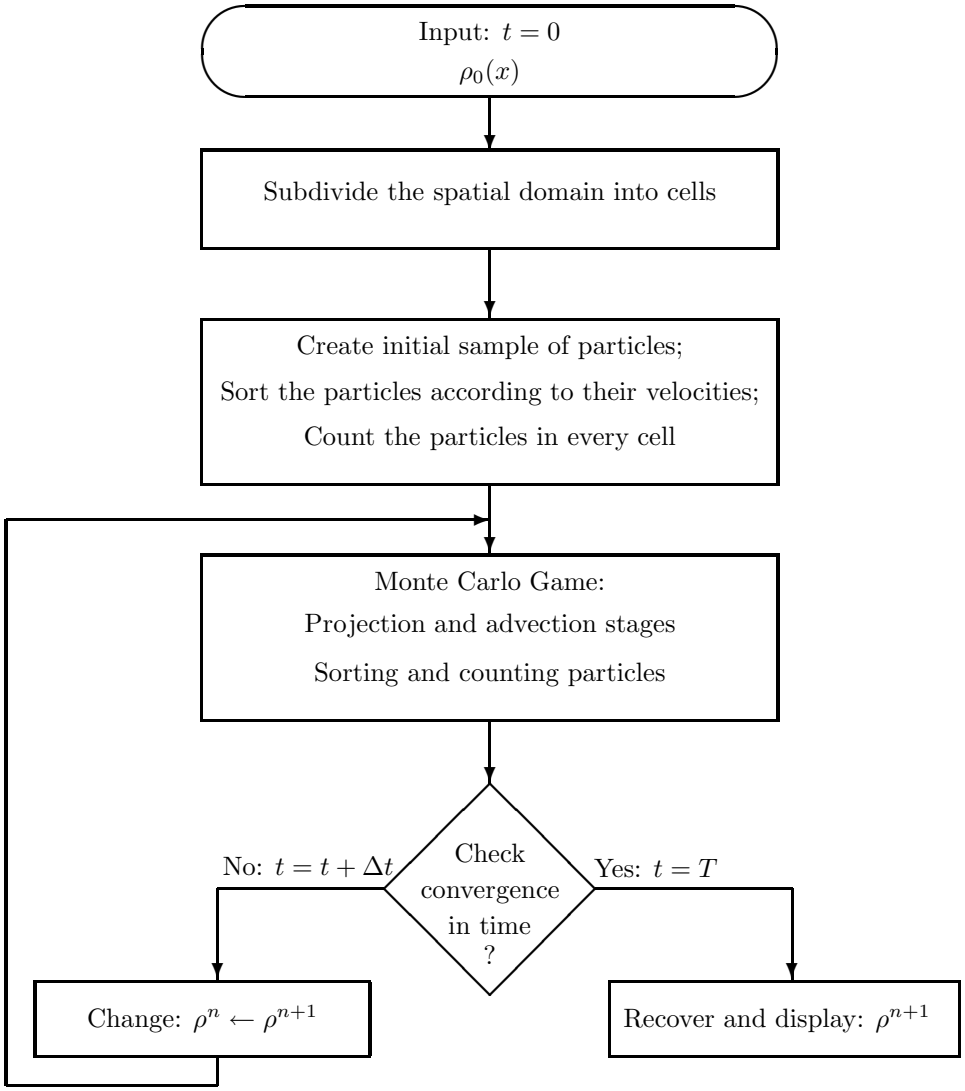

FIGURE 1. Flow chart of Monte Carlo approach for traffic flow problems.

where ρ_0 is the initial data and $n(x_i, t)$ is the number of the particles located in the cell I_i at time t. For comparison reasons, we also include results obtained for the system (10)-(11) using the deterministic relaxation scheme developed in [10].

5.1. **Example of Free Traffic.** We solve a free traffic situation corresponding to the following initial condition

$$\rho_0(x) = \frac{1}{\sqrt{2\pi}} e^{-\frac{3}{2}\left(x+\frac{5}{2}\right)^2}. \tag{40}$$

This condition corresponds to a vehicle-density normally distributed around the point $x = -2.5$ in the computational domain. Advancing the time, vehicles are

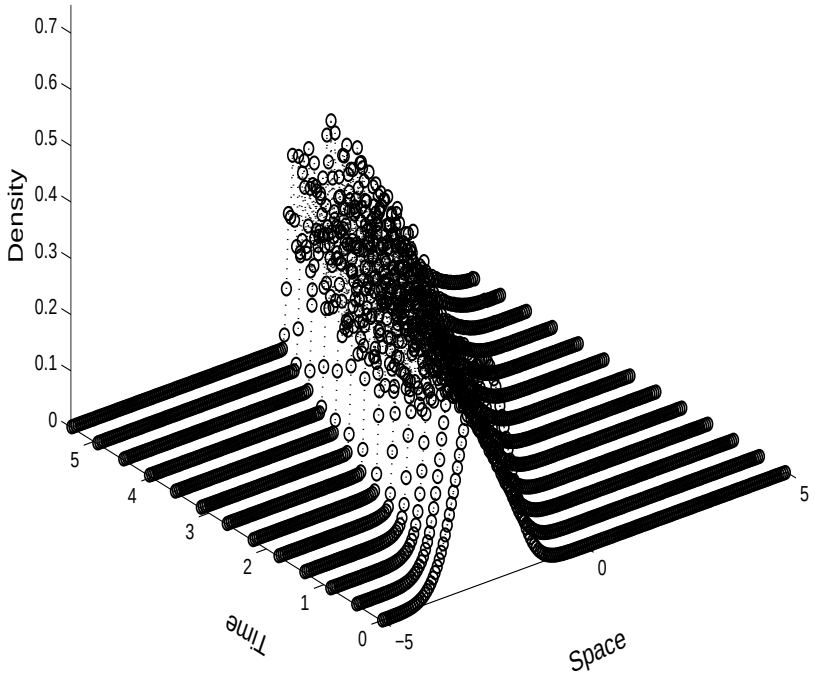

FIGURE 2. Evolution of density in the free traffic case.

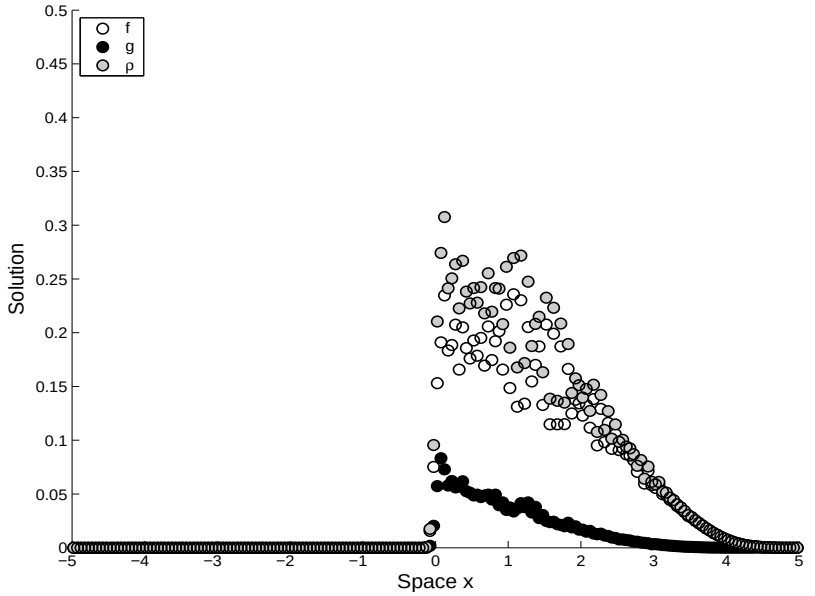

FIGURE 3. The kinetic variables f and g at $t = 5$ for the free traffic case.

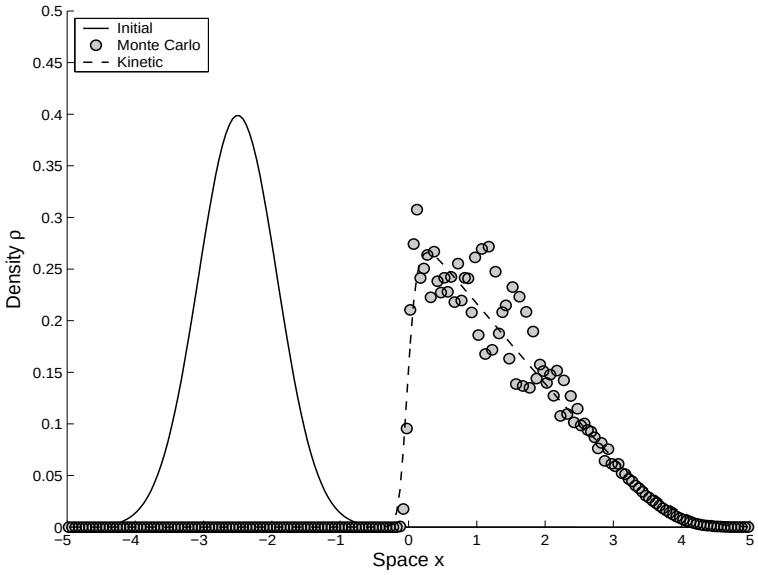

FIGURE 4. Computed results at $t = 5$ for the free traffic case.

allowed to freely move with speeds v_1 and v_2 according to the Monte Carlo algorithm described in the previous section. In Figure 2, we display the evolution of vehicle density in the time-space domain. As can be seen, the density distribution is freely advected in the flow direction within the time simulation. The oscillations observed in the computed results are due to the stochastic effects and are part of any Monte Carlo procedure. These stochastic fluctuations can be damped out by increasing the number of particles or plotting the mean density of a set of performed realizations as it is commonly used in statistical methods.

In Figure 3, we present the profile of the kinetic variables f and g at time $t = 5$. According to their speeds, the kinetic variables f and g are distributed in the computational domain and the computed density results from their sum. In order to compare our results to the deterministic method [10], we show in Figure 4 the computed results along with the initial data. It can be seen that the free transport behavior is accurately captured by the discrete velocity model. The presented Monte Carlo method advects the initial density profile without either numerical diffusion or oscillations in the computed density.

5.2. **Example of Traffic Jam.** Next we consider a traffic jam situation. The initial density for this example is given by

$$\rho_0(x) = \begin{cases} \dfrac{1}{\sqrt{2\pi}} e^{-\frac{3}{2}\left(x+\frac{5}{2}\right)^2}, & \text{if} \quad x \le 1, \\ 1, & \text{elsewhere.} \end{cases} \tag{41}$$

Here, additional to a vehicle-density normally distributed around the spatial point $x = -2.5$, the spatial domain $[1, 5]$ is saturated ($\rho = 1$). This test case corresponds to a free traffic moving towards a congested traffic area. This is an interesting example from a practical view point. The evolution of vehicle density in time-space phase is displayed in Figure 5. The obtained results show the correct flow structure

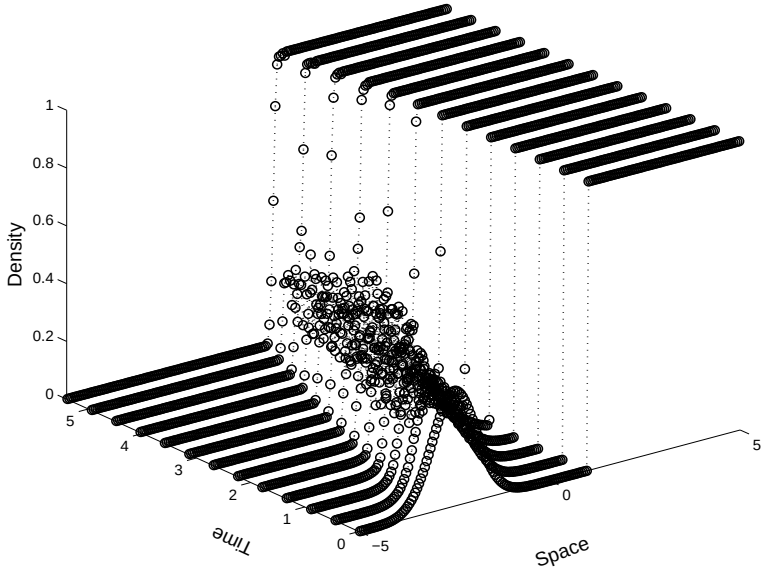

FIGURE 5. Evolution of density in the congested traffic case.

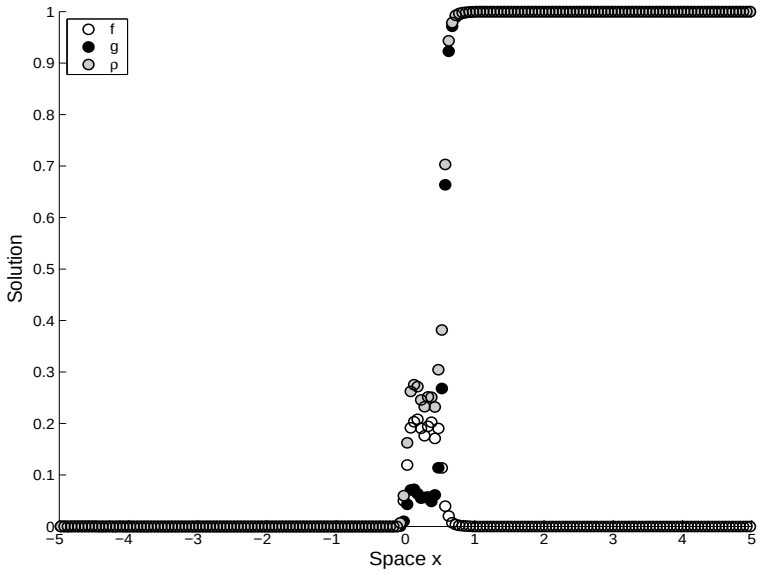

FIGURE 6. The kinetic variables f and g at $t = 5$ for the congested traffic case.

where the left vehicular density is freely transported till it reaches the traffic jam at $x = 1$. At this time a density wave is formed and advected backward, compare the jam position at the final time in Figure 5. Our model resolves this test case accurately and the shock is clearly captured.

In Figure 6, we plot the distribution of the kinetic variables f and g at time $t = 5$ when the backward wave is formed. It is clear that the variables f and g have been

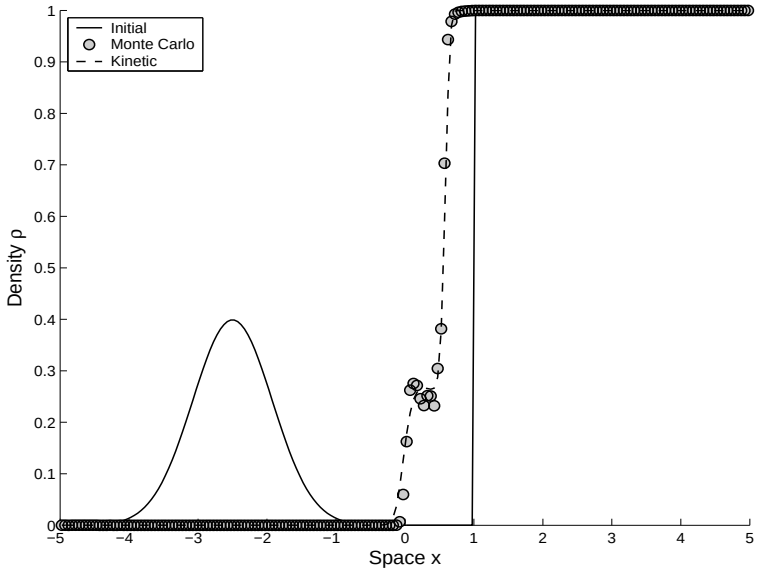

FIGURE 7. Computed results at $t = 5$ for the congested traffic case.

correctly distributed in the computational domain according to their corresponding speeds. For example, the kinetic variable f vanishes in the subdomain $[1, 5]$ where all the particles have speed v_1. Figure 7 depicts the comparison between the Monte Carlo results and those obtained using the deterministic method from [10]. Again, our Monte Carlo method reproduce accurate results without numerical dissipation or instability problems.

6. **Concluding remarks.** Kinetic discrete velocity models for vehicular traffic flow have been formulated and numerically solved. Consideration has been given to a two-speed model using the well-established LWR model for traffic flow in single road. The main advantage of the derived kinetic models is the fact that only nonnegative speeds are allowed in their formulations but still can recover backwards waves. This property coincides with the nature of traffic flow and is indispensable for modelling traffic flow using partial differential equations.

To solve the discrete velocity models we have proposed a probabilistic Monte Carlo method. The kinetic model and the Monte Carlo method have been validated for two situations in traffic flow. In both, free traffic and traffic jam situations, our approach correctly captures the traffic dynamics without diffusing the moving fronts or introducing non-physical oscillations. From these numerical tests one can conclude that the new approach yields results which are comparable than those obtained by deterministic methods. It should be pointed out that although we have restricted our study to the LWR model, our approach can also be used for more general traffic flow models like the AR model.

The vast applicability of the numerical tools for various traffic models is impressively evidenced in the engineering literature. Future work will focus on the extension of our approach for traffic flow in networks and also on its application to traffic flow models with stochastic flux functions. These stochastic effects may be originated from various inhomogeneities such as inhomogeneous road conditions,

weather conditions, traffic congestion managements, driver decisions among others. We believe that the discrete velocity model along with the Monte Carlo method presented in this paper can perform well for such problems.

Acknowledgments. The first and last authors would like to thank Department of Mathematics at Ferrara University where part of this work has been carried out. The authors also acknowledge the financial support by DAAD Vigoni Project D/06/19582.

REFERENCES

[1] F. Andrews and I. Prigogine, *A Boltzmann like approach for traffic flow*, Oper. Res., **8** (1960), 789–797.
[2] A. Aw and M. Rascle, *Resurrection of second order models of traffic flow?*, SIAM J. Appl. Math., **60** (2000), 916–938.
[3] R.E. Caflisch and L. Pareschi, *An implicit Monte Carlo method for rarefied gas dynamics I: The space homogeneous case*, J. Comp. Physics. **154** (1999), 90–116.
[4] G. Coclite, M. Garavello, and B. Piccoli, *Traffic flow on road networks*, SIAM J. Math. Anal., 36 (2005), 1862–1886.
[5] C.F. Daganzo, *Requiem for second order fluid approximations of traffic flow*, Transportation Research B, **29** (1995), 277–286.
[6] D. Gazis, R. Herman and R.Rothery, *Nonlinear follow-the-leader models of traffic flow*, Oper. Res., **9** (1961), 545–567.
[7] J. Greenberg, *Extension and amplification of the Aw-Rascle model*, SIAM J. Appl. Math., (2001), 729–745.
[8] D. Helbing, *Improved fluid dynamic model for vehicular traffic*, Physical Review E, **51** (1995), 3164–3169.
[9] D. Helbing, "Verkehrsdynamik," Springer-Verlag, Berlin, Heidelberg, New York, 1997.
[10] M. Herty, L. Pareschi and M. Seaïd, *Discrete Velocity Models and Relaxation Schemes for Traffic Flows*, SIAM J. Sci. Comp., **28** (2006), 1582–1596 .
[11] M. Herty and M. Rascle, *Coupling conditions for the Aw-Rrascle equations for traffic flow*, SIAM J. Math. Anal., **38** (2006), 595–616.
[12] M. Herty and A. Klar, *Simulation and optimization of traffic networks*, SIAM J. Sci. Comp., **25** (2004), 1066–1087.
[13] H. Holden and N.H. Risebro, *A mathematical model of traffic flow on a network of unidirectional roads*, SIAM J. Math. Anal., **26** (1995), 999–1017.
[14] A. Klar, R. Kühne, and R. Wegener, *Mathematical models for vehicular traffic*, Surv. Math. Ind., **6** (1996), 215–239.
[15] A. Klar and R. Wegener, *A hierarchy of models for multilane vehicular traffic I: Modeling*, SIAM J. Appl. Math., **59** (1998), 983–1001.
[16] M.J. Lighthill and J.B. Whitham, *On kinematic waves*, Proc. Royal Soc. Edinburgh (1955)
[17] L. Pareschi and M. Seaïd, *A New Monte-Carlo Approach for Conservation Laws and Relaxation Systems*, in "Computational science—ICCS 2004," Lecture Notes in Computer Science, **3037** (2004), 276–283.
[18] L. Pareschi and G. Russo, *An introduction to Monte Carlo methods for the Boltzmann equation*, ESAIM: Proceedings, **10** (2001), 35–76.
[19] H. Payne, *FREFLO: A macroscopic simulation model for freeway traffic*, Transportation Research Record, **722** (1979), 68–77.
[20] M. Schreckenberg, A. Schadschneider, K. Nagel, and N. Ito, *Discrete stochastic models for traffic flow*, Physical Review E, **51** (1995), 2939–2949.

Received February 2007; revised May 2007.

E-mail address: herty@mathematik.uni-kl.de
E-mail address: pareschi@dm.unife.it
E-mail address: seaid@mathematik.uni-kl.de